P300: The Similarities and Differences in the Scalp Distribution of Visual and Auditory Modality

Jun Ji*+, Bernice Porjesz*, Henri Begleiter*, and David Chorlian*

Summary: Purpose: To examine the topographic relationship of P3(00) between the visual and auditory modalities, especially to examine whether there are any modality-specific hemispheric differences of P3 in normal adults. Methods: The P3s were recorded from the same 41 normal right-handed males between the ages of 20 and 33 in both a typical auditory oddball task and a visual oddball paradigm with novel stimuli, with an extensive set of 61 scalp electrodes. In addition to the visual comparison and quantitative assessment of current source density (CSD) maps between the two modalities, canonical correlation analyses on the P3 raw amplitudes and examination of interaction effects of modality × location on both raw and normalized P3 data were performed. Results: The canonical correlation between modalities was generally high, especially at the left parietal brain region. There were no significant hemispheric effects in anterior brain but significant left-greater- than-right hemispheric effects in posterior brain regions in both modalities; modality-specific hemispheric effect was observed only at the parietal region. Strong surface current density activities were observed in the midline parietal-occipital area, and left and right boundary areas of temporal and inferior frontal region. Conclusions: The topographic similarities between P3s recorded in the visual and auditory modality outnumber the differences. Combining data from CSD assessments and profile analysis of P3 topography support the hypothesis of multiple generators of P3 that are differentially active in processing stimuli from different sensory modalities and are not symmetrically distributed between the two hemispheres.

Key words: Modality; P3 topography; Hemispheric; Current source density; Canonical correlation.

Introduction

P300 has received a wide range of research interest since it was first described by Sutton et al. (1965) as a positive-going component peaking around 300 msec after the eliciting event (cf: Bashore and van der Molen 1991; Polich and Kok 1995; Filipovic and Kostic 1995; Kugler et al. 1993; Morris et al. 1992). It is most commonly elicited in an oddball paradigm when subjects detect (mentally counting or button press) the occasional target stimuli (i.e., the oddball) in a regular train of standard stimuli. Its amplitude varies with the improbability of the targets, or the larger P300 results proportionally from the greater context changes (Picton 1992; Polich and Heine 1996). Its latency varies with the difficulty of discriminating the target stimuli from the standard stimuli, or the delay of the P300 reflects the prolongation of stimulus classification and/or evaluation time (Magliero et al. 1984; Coles et al. 1988). Its topographic profile shows a midline centroparietal-maximal scalp distribution (see Picton 1992). One defining feature of the P300 is its endogenous characteristic, i.e., no matter whether the eliciting stimuli are the same or not in terms of physical parameters, or whether they are in the same or different sensory modalities, the P300 can be elicited as long as the stimuli's task roles are equivalent.

The P300 has been elicited by stimuli not only from the auditory (Ramachandran et al. 1996; Fein and Turetsky 1989) and visual (Gratton et al. 1990; Sangal and Sangal 1996) modality, but also from the somatosensory modality (Yamaguchi and Knight 1991; Barrett et al. 1987). Furthermore, Naumann et al. (1992) found no influence of modality on the P300 elicited by rare stimuli when the P300 between the auditory and visual modalities were compared, asserting that modality independence is an important aspect of an endogenous component like the P300. However, Johnson (1989a) claimed that his study in 40 normal females between the ages of 7 and 20 had provided compelling evidence that P300 activity is not independent of the modality of the eliciting stimulus. The effect of modality on P300 re-

*State University of New York, Health Science Center at Brooklyn, NY, U.S.A.

+Institute of Mental Health, Beijing Medical University, Beijing, China.

Accepted for publication: December 5, 1998.

Supported by NIH Grants: AA05524 and AA02686. The authors wish to thank Arthur Stimus, Brian Beckrich, Elisabeth Iskander and Vladimir Kotlyarevsky for their valuable assistance.

Correspondence and reprint requests should be addressed to: Dr. Bernice Porjesz, Department of Psychiatry, Box 1203, SUNY, HSCB, 450 Clarkson Ave. Brooklyn, NY, 11203, USA.

Fax: (718) 270-4081

E-mail: bp@bp.cns.hscbklyn.edu

mained unresolved despite its unique contribution to our understanding of P300 generators.

Compared to other efforts, such as scalp EEG recordings in brain-lesioned subjects, or intracerebral recordings (Baudena et al. 1995), analyses of scalp P3 recordings in normal subjects from different modalities will also illustrate the brain structures of P300 generation. Simson et al. (1977) descriptively compared the modality similarity of the scalp distributions of the P3 (and N2) by calculating the Pearson correlation coefficient (γ) from pairs of grand mean amplitude measures at 13 scalp locations from 8 normal subjects. They reported that the visual P3 was widely distributed with a parietal maximum, resembling the topography of the auditory P3 (γ=0.86); they concluded that the P3 was not modality specific in its topographic distribution. Snyder, Hillyard, and Galambos (1980) quantitatively assessed percentage distributions (a percentage of amplitude at Cz for each subject) of the P3 amplitude across the scalp among different modalities by not only considering intercorrelation data but also evaluating the interactions of modality × scalp site (9 scalp sites); they found that the scalp distributions of P3s revealed no substantial differences among visual, auditory, and somatosensory modalities despite some marginally significant interactions at lateral electrode sites, which had been regarded as type I errors.

These early studies utilized relatively less sophisticated methods to assess scalp distribution of ERP between modalities in comparison to methods recommended by McCarthy and Wood (1985). In their influential publication, McCarthy and Wood (1985) claimed that there is an ambiguity posed by interaction analysis involving electrode locations, namely the incompatibility between the additive ANOVA model and the multiplicative effect on ERPs produced by changes in source strength. A practical solution is to find a proper scalar to eliminate amplitude differences between conditions and focus on differences in the shape or pattern of voltage differences across electrode locations. Although both studies employed normalization procedures, the works of Johnson (1989a,b) and Naumann et al. (1992) did not lead to a convergent conclusion in terms of modality dependence / independence of P300. Haig et al. (1997) recently cast reasonable doubt on the validity of normalization scaling in assessing topographic difference between conditions. They argued that since scaling introduces as many problems as it solves, for the sake of a reliable interpretation the unscaled analysis should always be reported in addition to the scaled analysis (Haig et al. 1997).

However, to determine whether the scalp topography of P3 possesses modality-specific characteristics as well as hemispheric differences, data from a more comprehensive set of electrode sites need to be collected. A full description of the spatial distribution relies somewhat on dense spatial sampling (Tucker 1993). One direct advantage of employing more electrodes is that each traditionally separated brain region (which is necessary for the understanding of scalp topography) can be represented by the vector of a group of electrodes instead of being represented by a single locus in that region. None of the above studies has employed a full complement of the 21 electrodes of the 10/20 International system. The relatively sparse electrode coverage in these studies was not adequate to address the topographic relationships of P300 between modalities. Recent studies by R.B. Sangal and J.M. Sangal (1996) employed 31 scalp electrodes to describe the topography of auditory and visual P300 in normal adults; they reached the conclusion that significant topographical differences in P300 amplitudes by modality or by hemisphere were not evidenced in MANOVAs of raw amplitudes, nor in ANOVAs of the mean of the raw amplitudes.

Yet studies which applied P300 in clinical populations have indicated that the sensitivity of visual P300 to the alcohol-related neural aberrance appeared to be more consistent than that of auditory P300 (see Ramachandran et al. 1996), while auditory P300 appeared more sensitive to the information processing dysfunction in chronic tinnitus patients (Attias et al. 1996) and schizophrenics (Ford et al. 1994; Squires-Wheeler et al. 1993) than visual P300. Like many terms employed in neuroscience, the concept of P300 evolved in complexity as more microstate-related subcomponents became detectable with various manipulations of stimulus paradigm (Katayama and Polich 1996a,b; Courchesne et al. 1978). Thus it is of practical importance to expand investigations on the relationship between visual and auditory P300s in healthy subjects, with confounding factors (such as intra-paradigm stimulus relationships, stimulus difficulty and task context) being taken into account (Comerchero and Polich, in press).

It is the purpose of the present study to expand the investigation of the topographic relationship of P300 between auditory and visual modalities (with more extensive set of recordings: 61 scalp electrodes based on the International 10-20 system). Both raw data analysis and standard normalization (MinMax) procedure will be employed in this study. Furthermore, in order to visualize the modality-specific / nonspecific topography of P300, current source density (CSD) map and ERP map are going to be employed as well. Finally, according to Salisbury et al. (1996), lateral or overall P3 reduction may associate correspondingly with the diathesis or potential confounds of schizophrenia, yet modality-specific hemispheric differences of P300 in normal adults has not received as much attention as did the issue of global

modality-specific difference. Thus, we are also interested in examining whether there are any hemispheric differences of P300 as well as whether the hemispheric pattern is modality-specific in normal adults.

Methods

Subjects

Forty-one adult male participants (24.53 ± 3.27, between 20-33 yrs old) were recruited either through newspaper ads or notices posted in the Health Science Center. They were paid for their participation. None of them has reported any history of neurological or psychiatric disease on a screening questionnaire. All subjects were right-handed and had normal or corrected normal vision. Males were used exclusively to maximize the likelihood of obtaining cognitively based hemispheric differences (Halpern 1992).

Recording procedure and stimuli

EEG activity was recorded monopolarly using a 61-lead electrode cap (Electro-cap International, Inc.) referred to the nose and grounded with a forehead electrode. The vertical and horizontal EOG were recorded, and ocular artifact rejection (>73.3 uv) was performed on-line. The impedances were kept below 5 kΩ, and the signals were amplified 10K (Sensorium EPA-2 Electrophysiology Amplifiers). Electrical activity was sampled continuously at a rate of 256 Hz (bandwidth: 0.02 to 50 Hz), and digital filtering (32-Hz low-pass filter) of the raw data was performed offline.

The subject was seated in a reclining chair located in a sound-attenuated RF shielded room (IAC) and fixated a point in the center of a computer display located 1m away from his eyes. The designation of the sequence of the modalities (visual first or auditory first) was alternated across subjects.

To elicit an auditory P3, the subject was presented with up to 400 binaural stimuli with uniform ISI of 1500 msec. There were two types of stimuli: a 600 Hz low tone and a 1600 Hz high tone. Each stimulus had a 60-msec duration (10 msec rise/fall, 40 msec plateau) and an intensity level of 60 dB SPL. The rare and frequent (standard) tones had 12.5% and 87.5% probabilities of occurrence, respectively. The designation of the low or high frequency tone as the rare stimulus was alternated across subjects. The auditory stimuli were presented binaurally through headphones (Etymotic Research, model ER-3A Tubephone Insert Earphones, 50Ω impedance), in which the ear piece and a short length of the Tubephone were fitted under the electrode cap, and the individual left and right transducer cases were situated on either side of the neck.

Visual P3s were elicited with 280 stimuli presented on a computer monitor for a duration of 60 ms, with an interstimulus interval of 1.6 s. The target (12.5% of total stimuli) was a white " X" (4 × 4 cm, 2.9° × 2.9°), standard nontarget (75%) was a white square (4 × 4 cm, 2.9° × 2.9°), and novel stimuli (12.5%) consisted of non-repeating colored geometric shapes (5 × 5 cm, 3.6° × 3.6°) arranged in variegated patterns.

Subjects were instructed to press a key pad with their forefinger (response hand was counterbalanced across subjects) whenever a target was detected, and to refrain from responding when the novel or standard stimuli occurred. The button-press action terminated a clock started at stimulus onset and defined the response time. The auditory experiment could be terminated after as few as 100 artifact-free trials (a minimum of 25 target and 75 nontarget trials) were acquired. The visual experiment terminated automatically after a minimum of 25 target stimuli, 150 nontarget stimuli, and 25 novel, artifact-free trials had been acquired, or when all 280 stimuli had been shown. The total length of the ERP epoch was 1500 msec for the auditory paradigm, and 1620 msec for the visual paradigm, including a prestimulus baseline of 187-msec. Trials (both visual and auditory paradigms) with response times > 1000 msec were rejected. The ERPs from accepted trials were automatically placed in target, novel (visual only), and nontarget response categories for subsequent summation, averaging, and statistical analysis. Response speed was emphasized, but not at the cost of accuracy.

Data analysis

A semi-automatic peak detection program was employed to analyze the average ERPs to target, standard nontarget, and novel (visual only) stimuli. The auditory P3 was selected as the largest amplitude peak within a time window from 215 to 430 msec. The visual P3 was selected as the largest amplitude peak within a time window from 215 to 530 msec. The amplitudes were measured at the peak with respect to a 125-msec prestimulus baseline. Latencies were measured from the time of the stimulus onset to the peak of each component. Because the main purpose of this research was focused on the characteristics of P300 between modalities, analyses involving visual novel stimuli elicited P3, as well as other ERP components, will not be reported here. Due to space limitations, grand mean ERPs at only 3 (of 61) electrodes over the scalp (Fz, Pz, Cz) elicited by target and nontarget stimuli for both modalities are illustrated in figure 1 (the upper two rows); the bottom row in figure 1 shows the grand mean ERPs evoked by the auditory target stimuli superimposed on those evoked by the visual target stimuli.

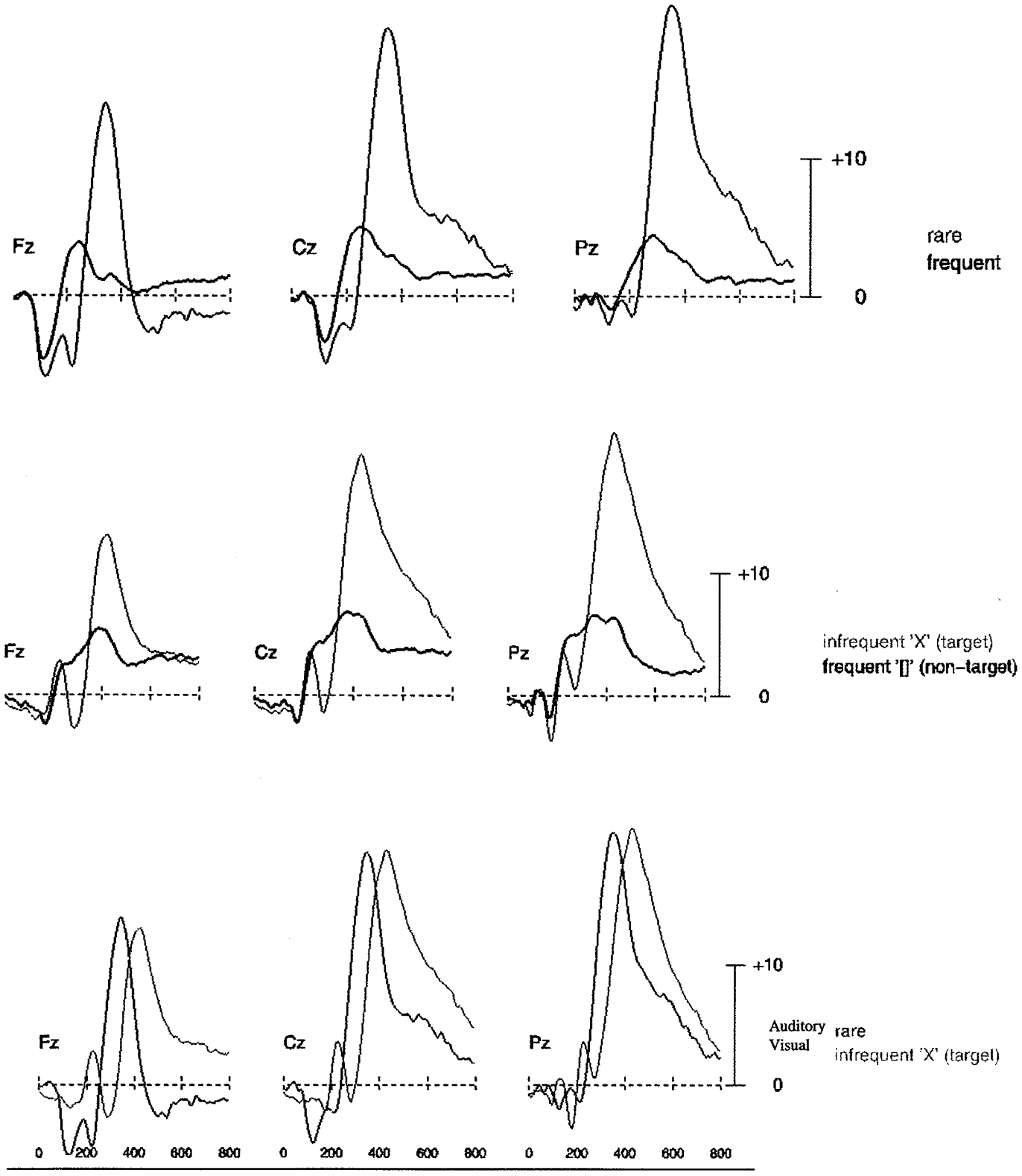

Figure 1. Grand mean ERPs of P3s over 3 scalp sites (Fz, Cz, Pz), nose reference. The upper row presents auditory responses, the middle row visual responses, and the bottom row presents auditory and visual target responses.

ERP data were analyzed for specific electrodes and regional groups of electrodes, because both individual and regional differences between modalities were of interest. Statistical analyses of ERP data were only conducted on artifact-free trials with correct behavioral responses. Five regional groupings of the 61 electrodes were created for regional analysis. The frontal region consisted of FP1/2, FPZ, AF7/8, AF1/2, AFZ, F7/8, F5/6, F3/4, F1/2, FZ; the central region consisted of FC5/6, FC3/4, FC1/2, FCZ, C5/6, C3/4, C1/2, CZ; the parietal region consisted of CP3/4, CP1/2, CPZ, P3/4, P1/2, PZ; the occipital region consisted of PO7/8, PO1/2, POZ, O1/2, OZ; the temporal region consisted of FT7/8, T7/8, TP7/8, CP5/6, P7/8, P5/6. Further regional grouping was organized into midline, left or right side of the scalp on each aforementioned region.

We chose canonical correlation (SAS v6.09: CANCORR Procedure) to describe the similarity between auditory and visual P3s on the raw P3 amplitudes at the aforementioned 5 brain regions. Canonical correlation is a technique for analyzing the relationship between two sets of variables (visual P3 amplitudes and auditory P3 amplitudes, in this case). Each set may contain several variables (i.e., P3 amplitudes among 12 temporal electrodes). Thus instead of yielding a correlation between auditory P3 and visual P3 at a single electrode (e.g., T7) of a brain region, we calculate the canonical correlation of each brain region (group of electrodes).

To enhance the validity of comparisons across modalities, all P3 amplitudes were normalized by the Min-Max procedure similar to that employed by Naumann et al (1992). The minimum and maximum grand mean P3 amplitudes were found in each of the two data sets (auditory target: Max_Pz: 23.68 uv, Min_AF8: 7.51 uv; visual target: Max_Pz: 23.34 uv, Min_FP1: 7.52 uv). The minimum grand P3 amplitude was subtracted from the raw amplitude at each location, then divided by the difference between maximum and minimum amplitudes. MANOVAs (SAS v6.09, PROC GLM) was used to assess the effects of modality (auditory, visual), hemisphere (left, right) on P3 amplitude and latency of the chosen electrodes or the regional group of electrodes. In addition, two kinds of topographic map were created by employing a reference-free model (see Wang et al. 1994; Perrin et al. 1989), where the ERP maps were plotted by interpolating the average reference data using the spherical spline method, while the current source density (CSD) maps were obtained by taking the second spatial derivative of the voltage fields. The CSD is thought to be more precise than the ERP in reflecting the cortical electrical activity under the scalp (see Ramachandran et al. 1996).

Results

Temporal data

Subjects took a significantly longer time [$t(41) = -7.11$, $p < .0001$] to respond correctly to the visual targets (452.18 ± 75.67 msec) than to the auditory targets (377.35 ± 68.79 msec). The latencies (21 sites of 10/20 system) of recorded P3 also differed significantly between the visual and auditory modalities [$F(21, 60)=11.64$, $p< .0001$]. For example, at Pz, where the largest P3 is recorded, it is clear that the above effect was due to the fact that visual P3 latency (426.70 ± 31.50 msec) was significantly later than the auditory P3 latency (348.77 ± 29.67 msec). MANOVA of P3 latencies with hemisphere (excluding the midline electrodes) as one repeated effect revealed no significant main effect of hemisphere, nor any interactions involving hemisphere and modality. In accord with the response time data and latency data, the topographic voltage maps in figure 2 illustrate the appearance-apex-withering process of the overwhelming parietal - concentric posterial P300 field activities, with different time courses involved in visual and auditory modalities.

Similarity: visual and auditory P3

The P3 waves elicited by targets in the visual and auditory modalities are very similar (figure 1) in their scalp distributions. The canonical analysis on the amplitudes of auditory and visual P3 were conducted at each brain region. Table I summarizes the first canonical correlations of the auditory P3 and visual P3 recorded at the same set of electrodes and the first canonical correlations of P3 amplitudes at the left electrodes and their corresponding right sites, as well as the probabilities at which the current canonical correlations are zero. The correlations of target P3 are uniformly high, larger than .70, and they are all statistically significant ($p<.0001$), indicating that there are strong similarities among the topographic distributions between the two modalities. The largest canonical correlations for targets were those obtained from the parietal regions, with the left parietal electrode configuration (including CP1, CP3, P1, and P3) yielding the largest correlation. The correlations between the left and right electrode configuration within each modality were all greater than .88; the inter-hemispheric correlations in the posterior region (occipital and temporal sites) were lower in both visual and auditory modalities than the inter-hemispheric correlations in the anterior brain regions (table I).

The quantitative assessment of the CSD maps (figure 4: auditory_347 msec vs. visual 425 msec) in different modalities also yields very high Z estimators — 0.93; the Z estimators were calculated, as proposed by Desmedt and Chalklin (1989), as an index expressing the instanta-

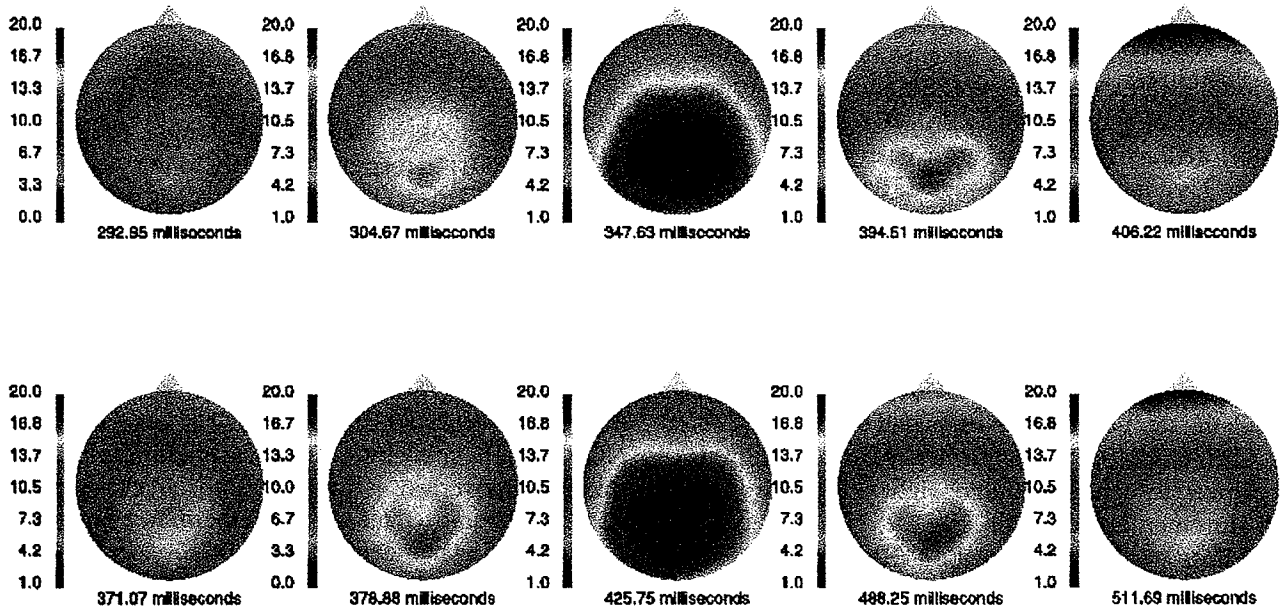

Figure 2. ERP maps over 5 time points centered around the peak latency. The upper row presents auditory target responses, the bottom row presents visual target responses.

neous topographic congruities of two maps by a number between 1 (identical) and -1 (reversed topographic pattern). Each set of measures at the n scalp electrodes (2881 interpolating CSD data for each map in this case) was interpreted as a resultant vector in a space with n dimensions, the cosine of the angle between the two corresponding vectors in that space was therefore calculated for the Z estimator. This high Z value suggests a highly similar surface brain electrical activity under the peak P3 component between the auditory and visual modality.

Difference: visual and auditory P3

To get the overall scalp distribution patterns for the visual and auditory P3, the analyses of variances were first applied to three subgroups of 61 electrodes (9 for the midline set, 26 for the left, 26 for the right), and a full complement of electrodes according to the 10-20 system. The results of MANOVA performed on raw amplitudes and the normalized data are given in table II. The modality differences of P3 are statistically significant only among the 26 scalp sites of the right hemisphere; this modality difference is also dependent on the recording sites (significant interaction of modality × location) (see table II). Before going further in comparing the amplitude difference, the possible confounding effect of the significant sensory-temporal gap between modalities on the difference pattern of visual P3s and auditory P3s should be considered. We added the response time (RT) as a

Table I. The results of canonical correlation analysis. The canonical correlation of P3 amplitudes between auditory and visual modality was calculated for each brain region respectively. **L/R_au:** refers to the correlation that was calculated from corresponding left and right electrodes in auditory modality, **L/R_vi:** refers to the correlation that was calculated from corresponding left and right electrodes in visual modality.

The first canonical correlation (*:p<.01, **:p<.001) of P3 amplitudes (auditory_au with visual_vi).					
LOCATION	Frontal	Central	Parietal	Occipital	Temporal
Midline	.71**	.79**	.92**	.74**	
Left	.84**	.86**	.93**	.72**	.90**
Right	.87**	.85**	.87**	.64**	.79**
Left/Right_au	.99**	.99**	.99**	.94**	.92**
Left/Right_vi	.99**	.99**	.97**	.92**	.88**

Table II. The regional MANOVA results performed on both raw and normalized P3 amplitude data; the results with reaction time as a regression variable are presented in the shaded cells.

F values of regional MANOVAs (*:p<.05, **:p<.01, ***:p<.001.								
	Midline 9 locations		Left 26 locations		Right 26 locations		10/20: 21 locations	
	Raw	MinMax	Raw	MinMax	Raw	MinMax	Raw	MinMax
Location (L)	116.94***	117.30***	31.51***	31.55***	38.49***	38.33***	45.76***	45.71***
◊	11.58***	11.64***	3.98***	3.98***	4.34***	4.33***	6.58***	6.59***
M × L	0.85	0.88	1.38	1.37	2.53**	2.56***	1.73	1.72
◊	0.57	0.69	1.47	1.49	1.91*	1.97*	2.23*	2.31*
Modality (M)	0.75	0.78	1.31	1.30	2.39**	2.41**	1.66	1.65
◊	0.52	0.62	1.39	1.42	1.81*	1.86*	2.12*	2.19*

◊: F values with reaction time as regression variable.

regression variable into the above analyses (see table II): the significant effects obtained on the right hemisphere remained significant, with significant response time regression effects [F(1,79) = 6.05_raw / 6.12_norm, p<.05] in the absence of significant response time × location effects. The regression of response time did not change significance levels of the modality effects in the midline and left scalp sites; however the 21 scalp sites of 10/20 system yielded significant modality as well as modality × location effect, with significant regression effects of response time [F(1,79) = 5.87_raw / 5.92_norm, p<.05] as well as significant response time × location effects [F(15,65) = 2.32_raw / 2.33_norm, p<.05]. These results (viz. results with or without RT as regression variable) indicate that the temporal processing gap between different sensory modalities do influence the overall scalp distribution patterns for the visual and auditory P3.

Both the canonical analyses and the variance analyses revealed that the P3 evoked by visual and auditory targets was not prominently different at the left scalp electrode locations while it was significantly different at the right scalp electrode sites. Thus further cross-modality MANOVAs with hemisphere as one of the within-subjects factor was performed on P3 amplitude (MinMax) arrays of each of the five brain regions; the results are summarized in table III. At the frontal and central region (figure 3a, b and table III), there was no sign of symmetric or asymmetric difference between auditory and visual modality (no significant hemisphere × modality effect), nor any asymmetric sign for either auditory or visual P3 (no significant hemisphere effect). There was a significant interaction effect of hemisphere × modality at the parietal region (see table III, though neither main effect of hemisphere nor main effect of modality was significant). Figure 3c revealed this interaction effect in the parietal region: P3s appeared smaller at the left sites than at the right sites in the auditory modality while this hemispheric pattern appeared opposite in the visual modality. At the occipital and temporal regions (see table III), in the absence of an interaction effect of hemisphere × modality, there was a significant main effect of hemisphere; figure 3d and figure 3e indicate that P3s at left scalp sites were larger in general

Table III. The regional MANOVA results performed on normalized P3 amplitudes with hemisphere as one repeated measure.

Cross-modality MANOVA of P3 amplitude_MinMax for the five scalp regions (F value).					
p<.05*	Frontal	Central	Parietal	Occipital	Temporal
p<.01**	7 electrodes	6 electrodes	4 electrodes	3 electrodes	6 electrodes
p<.001***	on each side	on each side	on each side	on each side	on each side
Hemisphere (H)	0.002	0.55	0.009	13.05***	4.60*
H × M	0.21	0.98	4.51*	1.39	0.76
H × Location (L)	0.63	0.99	2.16	1.15	3.94**
H × L × M	0.57	0.95	1.20	0.19	0.89
Modality (M)	0.01	0.00	0.12	1.39	2.16

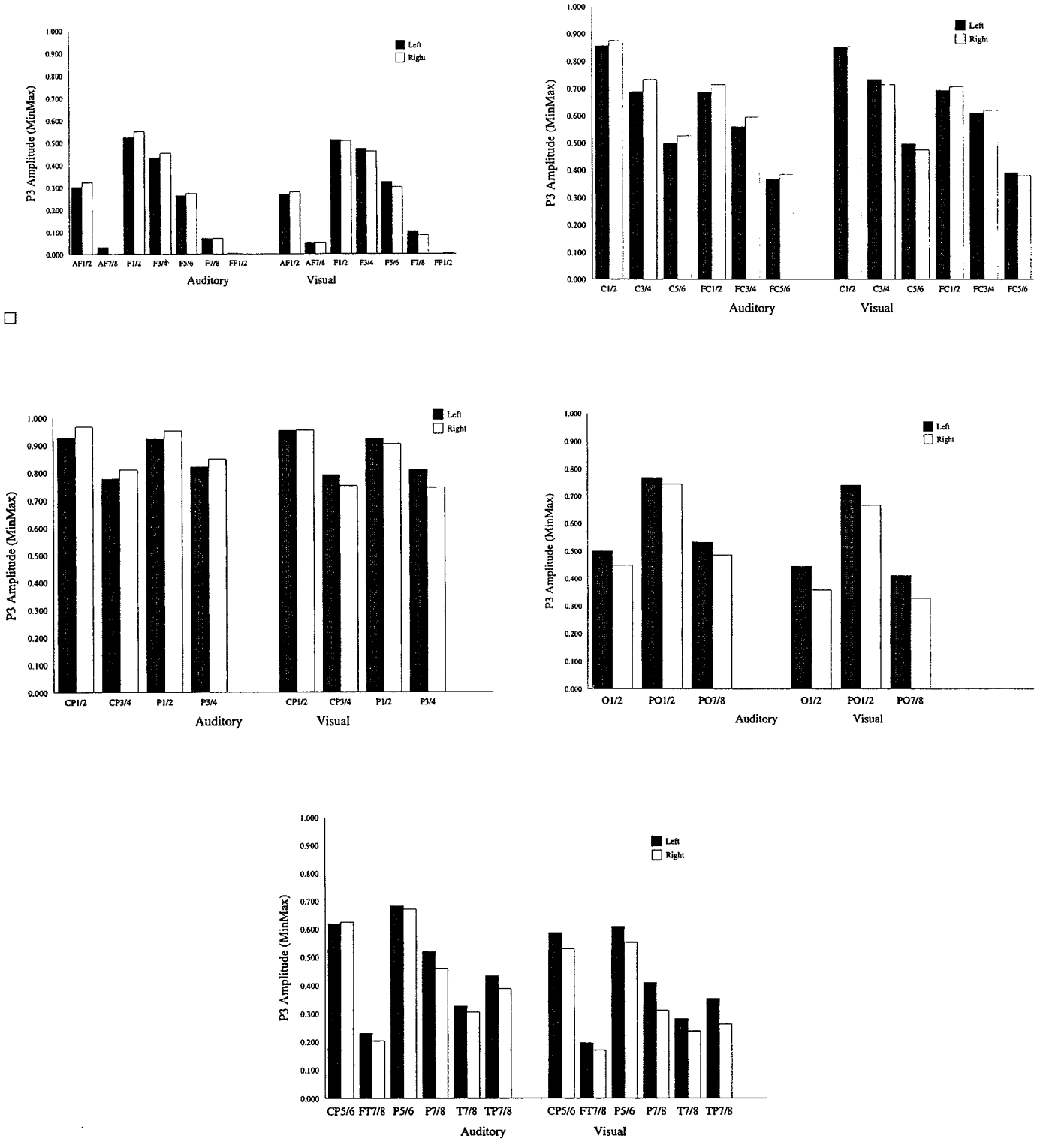

Figure 3. Histogram of P3 amplitude (MinMax) at each electrode of left and right hemisphere from both modalities, which was organized into Frontal (a) - top left, Central (b) - top right, Parietal (c) - middle left, Occipital (d) - middle right, and Temporal (e) - bottom, regions.

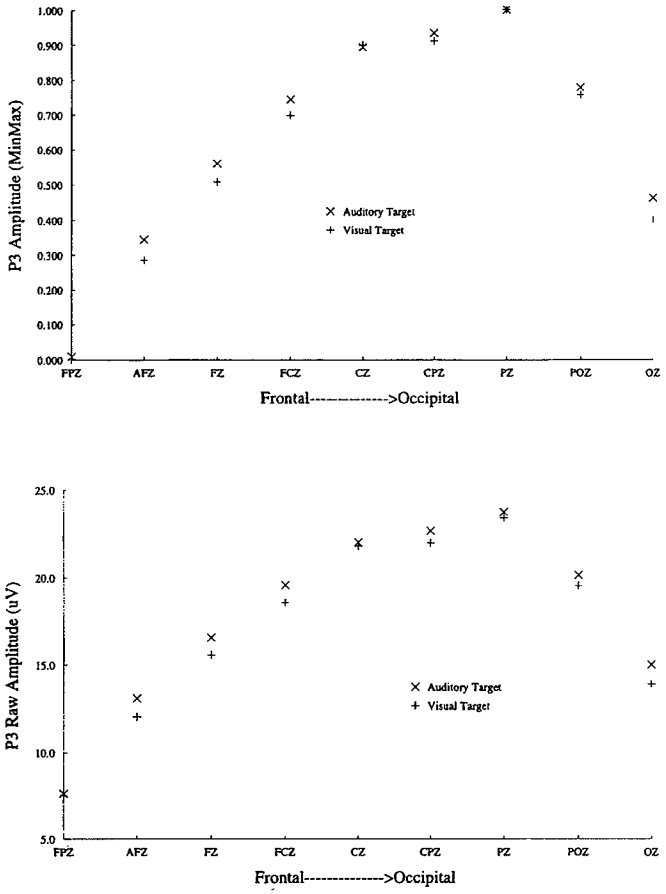

Figure 4. P3 normalized amplitude (a) - top, and raw amplitude (b) - bottom, along midline electrodes from anterior to posterior regions.

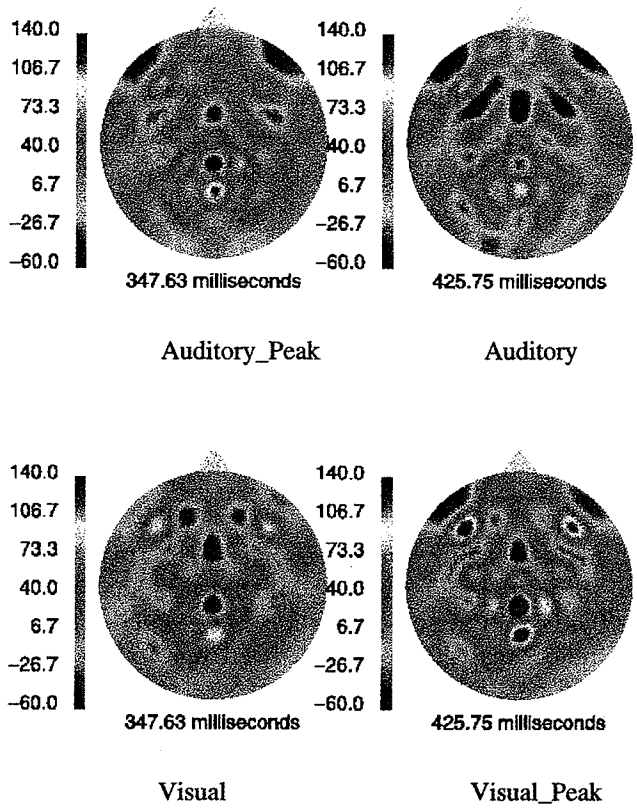

Figure 5. Current source density maps of target P3s at peak latencies of auditory modality and visual modality. The unit for the scale is $(uv/r^2)/cm^2$, r=radius of head.

than those at the right sites in both modalities. However, in the temporal region, there was also a significant interaction effect of hemisphere × location. Figure 3e reveals that the P3 hemisphere effect was not as graphically manifested at the CP5 /6 in the auditory modality as it was at the other sites.

The P3 distribution pattern along the sagittal midline scalp sites is demonstrated in figure 4. From the frontal toward the occipital region, target P3 in both modalities showed an increasing tendency, reaching maximal at the PZ, then decreasing along the occipital sites. Accordingly, MANOVA of target P3 amplitude (MinMax) at the 9 midline sites revealed a significant location effect [$F(8,73)=117.30$, $p<.0001$], no significant main effect of modality [$F(1,80)=0.16$, $p=0.69$], nor significant interaction effect [$F(8,73) = 0.88$, $p = 0.53$] of location × modality, which suggested that the target P3 was not distributed differently between auditory and visual modalities along the midline sites.

Visual and Quantitative Assessment of Topographic Maps

The CSD maps of P300 around the peak latency for auditory and visual modalities in figure 5 show a strong current source (over 100 uv/r2/cm2)-sink pair at midline parietal-occipital sites, with the sink anterior to the source. There was a sink-source-sink triplet at each of the inferior temporal frontal boundaries, much stronger in the visual modality, and slightly stronger on the left.

According to the visual assessment of the source-sink pattern, each CSD map was then further separated into frontal-central, parietal, and occipital-temporal regions for further quantitative evaluations. The quantitative assessment on regional CSD pattern was made possible by using a bootstrap method (Srebro 1996; Ji et al. in press) with modification. Initially, current density maps for each subject were calculated for 5 consecutive sample points centered around the peak latency derived from the grand mean ((samples 87-91 around auditory P3 peak latency (347 msec); samples 107-111 around visual P3 peak latency (425 msec)). The values were then averaged. Then 41 maps chosen randomly with replacement

Table IV. Pearson cross-correlation coefficients (Rs) between the left and right hemisphere and the Student T test results of Rs between the auditory and visual modalities.

Pearson cross-correlation coefficients (R: mean ± Std Dev).			
	Auditory_peak	Between modality t-test	Visual_peak
Whole head	.23 ± .11	t(315.3) = 13.6	.11 ± .07
		p < .0001	
Frontal-central	.02 ± .12	t(338.1) = 7.5	-.05 ± .07
		p < .0001	
Parietal	.24 ± .19	t(398) = -.68	.26 ± .18
		p > .05	
Occipital-temporal	.52 ± .16	NA	.38 ± .23

from the 41 subject maps were averaged. This was done 200 times to provide a basis for statistical analysis. The left vs. right Pearson correlation was calculated for each of the 200 maps for the whole head, and for the frontal-central, parietal, and occipital-temporal regions, and subjected to the Fisher Z transform, in order to apply Student's T-test to the values. To serve as the comparison in the Srebro method, 41 (half-) maps formed by randomly choosing the left or right half from the 41 subjects chosen randomly with replacement were averaged. This was done 200 times. Then the Pearson correlations between these 200 half-maps and their permutation without identities was taken on a whole head and regional basis and subjected to the Fisher Z transform (which we call the pooled Z values). To determine whether the metric of symmetry in the maps is statistically significant, a two-sample Student's T-test was applied to the left-right data and the pooled data. The left-right R's are significantly different ($p<.001$) from the pooled R's, except for the occipital-temporal region [auditory peak P3: $t(381) = 1.91$, $p > .05$; visual peak P3: $t(324) = -0.7$, $p>.05$]. The statistical significance is a necessary condition for the inter-modality comparisons. (If the R's are not different between the left-right and the pooled data then either the left and right data are close to identical or there is too much variability between subjects for any comparisons to have statistical significance.)

Table IV summarizes the mean and standard deviation of R's as well as the t-test results. The CSD map for the visual peak P3 revealed smaller R than that for the auditory peak P3, indicating a less symmetric pattern for the visual CSD map. Also, the difference of the R's between modalities are statistically significant in the anterior region while it is not in the posterior region, emphasizing the anterior contribution to the observed different symmetric pattern of CSD distribution between modalities.

Discussion

This study emphasized the scalp topographic relationship of P3s elicited by auditory and visual stimuli in the same 41 male adults; this relationship was quantitatively assessed by canonical correlations and interactions of modality × location. The canonical correlations among P3 amplitudes at different scalp regions between modalities were not equally high; the strongest similarity between modalities is obtained from the target P3 recorded at the left parietal sites as indexed by the largest value of the first canonical correlation. The modality similarity among the left parietal sites is confirmed by nonsignificant effect of modality × left electrode locations from analyses of variance of target P3 amplitudes. The topographic similarity between auditory and visual P3 components was further corroborated by the Z estimator. Since the Z estimator is sensitive to the similar or different sets of neural generators (see Desmedt and Chalklin 1989), the present near 1 Z estimator strongly suggests there are similar but not identical generator patterns underlying scalp recorded auditory and visual P3s. Further, both auditory and visual CSD maps showed similar symmetric patterns: the current density sources are more asymmetric in the frontal area while more symmetric in the occipital-temporal area.

Despite the strong similarities between auditory and visual P3, there were widespread significant modality effects which indicate that scalp distributions between the auditory and visual modalities are not identical. The visual target P3 in our study was elicited in a three stimulus paradigm while the auditory target P3 was obtained in a typical oddball paradigm. Previous reports (Katayama and Polich 1996a,b) have found that the target stimuli from 1-, 2- and 3-stimulus paradigm produced essentially the same P3 in the auditory modality, and it is more likely the task difficulty (target/standard discrimination) rather than the extra novel stimuli causes differ-

ences in target P3s among paradigms. Similarly, the different P3 topographic distributions between modalities in this study are not likely to be a reflection of the existence of the extra novel visual stimuli. To not detract from the topography comparison, the novel stimuli elicited P3 was not analyzed in this paper. However, our results suggest an influence of temporal gap between sensory processing on the modality effect and the effect of modality × location. The response time as the covariate actually signified a modality effect to some extent; that is, the modality effects are more pronounced after the temporal gap effect was taken out. According to Johnson (1989a,b), because modality differences in the shapes of profiles of P3 amplitude as a function of electrode location would indicate that more than one intracranial source contributes to the P3 for the two modalities, it was suggested that there are modality-specific bioelectric sources underlying P300 amplitudes. However, in Johnson's (1989b) study the significant modality × location effect was obtained from three midline sites (Fz, Cz, Pz) while in our study the midline sites (extended to 9 electrodes, see figure 3) did not reveal any significant modality related effect.

With regard to the midline P3 topographic distribution, our results are in accordance with Naumann et al.'s study (1992) which controlled type II error and employed three different normalization methods and still did not find the distribution over scalp of the P3 component varying with modality. Yet, different brain topography between auditory and visual P3s was also suggested from an experiment with implanted electrodes in monkeys (Pineda and Westerfield 1993): visual P3 responses were maximal over midline centroparietal sites while auditory responses were maximal over lateral sites. Our results indicate that modality-specific bioelectric sources may be more likely located on the right hemisphere since profile analyses of P3 amplitude yielded relatively stable modality and modality × location effect on the right brain scalp sites. While the similarity of auditory and visual P3 reflects the existence of modality - independent sources, the analyses of variance indicate the existence of modality-dependent sources.

In comparison to previous studies, we employed more electrode locations (61 electrodes) in the current data analysis, which not only allowed us to delineate the topographic relationship of P3 between visual and auditory modality in a much more comprehensive way, but also allowed the meaningful CSD comparisons. From the anterior to the posterior regions along the sagittal brain plane, similarities of topographic distribution of P3 between modalities outnumber the differences, as figure 4 demonstrates. The midline scalp distribution is not significantly different between the visual and auditory modality. Both auditory and visual P3 showed the expected parietal maximum distribution pattern; the further the scalp site is away from Pz, the smaller the P3 target amplitude at that site. While the midline distribution pattern of P3 from frontal to occipital sites may vary from experiment to experiment (Johnson 1993; Picton 1992), the most consistent feature is that the maximal P3 was usually recorded at Pz in both modalities (Polich and Heine 1996; Naumann 1992). The parietally maximal distributed P3 may not be a manifestation of the strong surface electric activity in the parietal-occipital area observed in the CSD maps, as similar surface electric activities in the lateral frontal temporal boundary area did not result in a proportionally larger frontal P3.

As to the P3 scalp distribution across hemisphere, the lateral pattern in the current data varied according to brain region, or to modality. While significant left-greater-than-right hemispheric effects were produced at the temporal and occipital sites in both modalities, no hemispheric differences for the P3 were produced at the frontal and central sites in both modalities. More importantly in the current data, is the finding of modality specific hemispheric effects (significant interaction of hemisphere × modality) at parietal sites, where the strongest P3 responses were recorded to targets — the stimulus condition which reliably elicits a prominent P3. Previous studies (Alexander et al. 1995; Alexander et al. 1996) mainly focused on within-modality hemispheric effects at specific loci; there it was claimed that right-dominant P300 amplitudes were observed primarily at anterior-medial locations (F3/4, C3/4) for both target and standard stimuli in both auditory and visual modalities, which is not completely consistent with the current hemispheric effects. In their studies, Fp1/2 (located in frontal area) and O1/2 (located in occipital region) were excluded from further consideration because of unreliable hemispheric effects; hemispheric effects at T7/8 and P7/8, which there represented lateral-central and lateral-parietal regions respectively, were not emphasized in their paper, but are somewhat consistent with our finding. They also observed left-greater-than-right hemispheric effects only for target stimuli at P7/8 sites, and right-greater-than-left hemispheric effects only for standard stimuli at T7/8 sites (Alexander et al. 1995, p. 471). P7/8 and T7/8 sites are loci contributing to hemispheric effect produced at the temporal region in the current data.

In addition, there was a significant right-greater-than-left hemispheric effect for target stimuli at P3/4 sites in the visual task (Alexander et al. 1995, p. 471) with no hemispheric effect for target stimuli at the same sites in the auditory task (Alexander et al. 1996, figure 2); this resembled the trend observed in the current results (left-greater-than-right in visual modality, right-greater-than-left in auditory modality) at the parietal region (CP1/2, CP3/4, P1/2, P3/4). However, the current hemispheric results

from anterior brain electrode sites (F3/4 and C3/4) differed from Alexander et al. (1996). As mentioned above, we did not find confirming evidence for a right-greater-than-left effect for target stimuli at anterior brain area as reported by Alexander et al. (1995, 1996). Our data did not support the finding that a simple, unanimous hemispheric pattern could be obtained that applies to all brain regions, or both visual and auditory modalities. Instead, the hemispheric asymmetries are likely varied as a function of modality and brain region.

There are inconsistences between current source activities and scalp-recorded electric activities in this study. First, there are no corresponding correlations between source-sink pairs and the amplitude of P3: no corresponding large P3 amplitudes were recorded at electrode sites around the strong source-sink pattern in the anterior area, even though the parietal source corresponded to the maximal P3 recorded at Pz. Second, the visual and quantitative assessment of CSD maps revealed similar asymmetric patterns for the auditory and visual modality; that is, for both modalities there are relatively symmetric current source activities in posterior regions with asymmetric current source activities in anterior regions. In contrast, P3 amplitude topographic analysis revealed asymmetry in the posterior region, but no asymmetry in anterior regions. The CSD maps were made using Spline Laplacian methods which are able to overcome problems in scalp-recorded ERP measurements such as: active reference, volume conductor effects, and contaminations by sources distant from the recording site (Nunez and Pilgreen 1991). Compared to the profile analysis of scalp-recorded P3, the CSD maps reflect more precisely the electrical activity under the scalp. Combining data from CSD assessments and profile analysis of P3 topography support the hypothesis of multiple generators of P3 (Holt et al. 1995) that are differentially active in processing stimuli from different sensory modalities and are not symmetrically distributed between the two hemispheres.

References

Alexander, J.E., Porjesz, B., Bauer, L.O., Kuperman, S., Morzorati, S., O'Connor, S.J., Rohrbaugh, J., Begleiter, H. and Polich, J. P300 hemispheric amplitude asymmetries from a visual oddball task. Psychophysiology, 1995, 32: 467-475.

Alexander, J.E., Bauer, L.O., Kuperman, S., Morzorati, S., O'Connor, S.J., Rohrbaugh, J., Porjesz, B., Begleiter, H. and Polich, J. Hemispheric differences for P300 amplitude from an auditory oddball task. International Journal of Psychophysiology, 1996, 21: 189-196.

Attias, J., Furman, V., Shemesh, Z. and Bresloff, I. Impaired brain processing in noise-induced tinnitus patients as measured by auditory and visual event-related potentials. Ear & Hearing, 1996, 17(4): 327-333.

Barrett, G., Neshige, R. and Shibasaki, H. Human auditory and somatosensory event-related potentials: effects of response condtion and age. Electroencephalography & Clinical Neurophysiology, 1987, 66: 409-419.

Bashore, T.R. and van der Molen, M.W. Discovery of the P300: a tribute. [Review] Biological psychology, 1991, 32(2-3): 155-171.

Baudena, P., Halgren, E., Heit, G. and Clarke, J.M. Intracerebral potentials to rare target and distractor auditory and visual stimuli. III. Frontal Cortex. Electroenceph. Clin. Neurophysiol., 1995, 94: 251-264.

Coles, M.G., Gratton, G. and Donchin, E. Detecting early communication: using measures of movement-related potentials to illuminate human information precessing. Biological Psychology, 1988, 26: 69-89.

Courchesne, E., Courchesne, R.Y. and Hillyard, S.A. The effect of simulus deviation on P3 waves to easily recognized stimuli. Neuropsychologia, 1978, 16: 189-199.

Comerchero, M.D. and Polich, J. P3a and P3b from typical auditory and visual stimuli. In press.

Desmedt, J.E. and Chalklin, V. New method for titrating differences in scalp topographic patterns in brain evoked potential mapping. Electroenceph. Clin. Neurophysiol., 1989, 74: 359-366.

Fein, G. and Turetsky, B. P300 latency variability in normal elderly: effects of paradigm and measurement technique. Electroencephalography & Clinical Neurophysiology, 1989, 72: 384-394.

Filipovic, S.R. and Kostic, V.S. Utility of auditory P300 in detection of presenile dementia. [Review] Journal of the Neurological Sciences, 1995, 131(2): 150-152.

Ford, J.M., White, P.M., Csernansky, J.G., Faustman, W.O., Roth, W.T. and Pfefferbaum, A. ERPs in schizophrenia: effects of antipsychotic medication. Biol. Psychiatry, 1994, 36(3): 153-70.

Gratton, G., Bosco, C.M., Kramer, A.F., Coles, M.G., Wickens, C.D. and Donchin, E. Event-related brain potentials as indices of information extraction and response priming. Electroencephalography & Clinical Neurophysiology, 1990, 75(5): 419-432.

Haig, A.R., Gordon, E. and Hook, S. To scale or not to scale: McCarthy and Wood revisited. Electroencephalography & Clinical Neurophysiology 1997, 103: 323-325.

Halpern, D.F. Sex differences in cognitive ablities. Hillsdale, NJ: Lawrence Earlbaum Associates, 1992.

Holt, L.E., Raine, A., Pa, G., Schneider, L.S., Henderson, V.W. and Pollock, V.E. P300 topography in Alzheimer's disease. Psychophysiology, 1995, 32: 257-265.

Ji, J., Porjesz, B., Chorlian, D. and Begleiter, H. Event-related potentials during digit recognition tasks. Cognitive Brain Research, 1998, in press.

Johnson, R. Jr. Developmental evidence for modality-dependent P300 generators: a normative study. Psychophysiology, 1989a, 26(6): 651-667.

Johnson, R. Jr. Auditory and visual P300s in temporal lobectomy patients: evidence for modality-dependent generators. Psychophysiology, 1989b, 26(6): 633-650.

Johnson, R. Jr. On the neural generators of the P300 component of the event-related potential. Psychophysiology, 1993, 30(1): 90-97.

Katayama, J. and Polich, J. P300 from one-, two-, and three-stimulus auditory paradigms. International Journal of Psychophysiology, 1996a, 23: 33-40.

Katayama, J. and Polich, J. P300, probability, and the three-tone paradigm. Electroenceph. Clin. Neurophysiol., 1996b, 100(6): 555-562.

Kugler, C.F., Taghavy, A. and Platt, D. The event-related P300 potential analysis of cognitive human brain aging: a review. [Review] Gerontology, 1993, 39(5): 280-303.

Magliero, A., Bashore, T.R., Coles, M.G.H. and Donchin, E. On the dependence of P300 latency on stimulus evaluation processes. Psychophysiology, 1984, 21: 171-186.

McCarthy, G. and Wood, C.C. Scalp distributions of event-related potentials: an ambiguity associated with analysis of variance models. Electroenceph. Clin. Neurophysiol., 1985, 62: 203-208.

Morris, A.M., So, Y., Lee, K.A., Lash, A.A. and Becker, C.E. The P300 event-related potential. The effects of sleep deprivation. [Review] Journal of Occupational Medicine, 1992, 34(12): 1143-1152.

Naumann, E., Huber, C., Maier, S., Plihal, W., Wustmans, A., Diedirch, O. and Bartussek, D. The scalp topography of P300 in the visual and auditory modalities: a comparison of three normalization methods and the control of statistical type II error. Electroencephalography & Clinical Neurophysiology, 1992, 83: 254-264.

Nunez, P.L. and Pilgreen, KL. The spline-Laplacian in clinical neurophysiology: a method to improve EEG spatial resolution. J. Clin. Neurophysiol., 1991, 8: 397-413.

Perrin, F., Pernire, J., Bertrand, O. and Echallier, J.F. Spherical splines for scalp potential and current density mapping. Electroenceph. Clin. Neurophysiol., 1989, 72: 184-187.

Picton, T.W. The P300 wave of the human event-related potential. [Review] Journal of Clinical Neurophysiology, 1992, 9(4): 456-479.

Pineda, J.A. and Westerfield, M. Monkey P3 in an "oddball" paradigm: pharmacological support for multiple neural sources. Brain Research Bulletin, 1993, 31: 689-696.

Polich, J. and Heine, M.R.D. P300 topography and modality effects from a single-stimulus paradigm. Psychophysiology, 1996, 33: 747-752.

Polich, J. and Kok, A. Cognitive and biological determinants of P300: an intergrative review. [Review] Biological Psychology, 1995, 41(2): 103-146.

Ramachandran, G., Porjesz, B., Begleiter, H. and Litke, A. A simple auditory oddball task in young adult males at high risk for alcoholism. Alcoholism: Clinical and Experimental Research, 1996, 20 (1): 9-15.

Salisbury, D.F., Voglmaier, M.M., Seidman, L.J. and McCarley, R.W. Topographic abnormalities of P3 in schizotypal personality disorder. Biological Psychiatry, 1996, 40: 165-172.

Sangal, B. and Sangal, J.M. Topography of auditory and visual P300 in normal adults. Clinical Electroencephalography, 1996, 27(3): 145-150.

Simson, R., Vaughan, J.R.H. and Ritter, W. The scalp topography of potentials in auditory and visual discrimination tasks. Electroencephalography & Clinical Neurophysiology, 1977, 42: 528-535.

Squires-Wheeler, E., Friedman, D., Skodol, A.E. and Erlenmeyer-Kimling, L. A longitudinal study relating P3 amplitude to schizophrenia spectrum disorders and to global personality functioning. Biological Psychiatry.1993, 33(11-12): 774-85.

Srebro, R. A bootstrap method to compare the shapes of two scalp fields. Electroencephalography & Clinical Neurophysiology, 1976, 100: 25-32.

Sutton, S., Braren, M., Zubin, J. and John, E.R. Evoked potential correlates of stimulus uncertainty. Science, 1965, 150: 1187-1188.

Synder, E., Hillyard, S.A. and Galambos, R. Similarities and differences among the P3 waves to detected signals in three modalities. Psychophysiology, 1980, 17(2): 112-122.

Tucker, DM. Spatial sampling of head electrical fields: the geodesic sensor net. Electroencephalography & Clinical Neurophysiology, 1993, 87(3): 154-63.

Wang, W.Y., Begleiter, H. and Porjesz, B. Surface energy, its density and distance: new measures with application to human cerebral potentials. Brain Topography, 1994, 6(3): 193-202.

Yamaguchi, S. and Knight, R.T. P300 generation by novel somatosensory stimuli. Electroencephalography & Clinical Neurophysiology 1991, 78(1): 50-55.